

sectional area approximately one-sixth of a normal renal or visceral lumen, providing significant leeway for mal-alignment. In light of this, we routinely use inflated balloons in the target vessels instead of sheaths during FEVAR deployment for the theoretical advantage of improved alignment. We also feel this simple maneuver may protect from atheroembolism during graft opening. The purpose of this study was to compare sheaths to inflated balloons for fenestration-to-target vessel alignment during deployment of a FEVAR bench top model with varying aortic configurations.

Methods: A 32 mm diameter Z-Fen proximal body (Cook Medical, Bloomington, Ind) was used for all test deployments. The device was configured with a single scallop (height 10 mm and width 10 mm) placed at the 12:00 position and two small fenestrations (height 8 mm and width 6 mm) placed 15 mm from the edge of the fabric and an arc length of 21.2 mm from the center of scallop on each side. Vinyl tubing with holes drilled to represent the superior mesenteric and renal arteries was used to create models of varying aortic anatomy. The vinyl tubing had an inner diameter of 25.4 mm. The superior mesenteric artery hole was 6.4 mm in diameter, and the renal artery holes were 5.6 mm in diameter. The position of the Z-Fen device in the vinyl tubing was controlled using string threaded through the struts of the proximal free-flow component and the most distal z-stent. A Newton wire was used to simulate the constraining wire and a short piece of plastic cylindrical tubing was used to simulate the top cap during the deployments. Three different aortic models were used. Model A was straight with holes drilled in perfect alignment with the fenestrated graft. Model B was designed to represent tortuous anatomy, the holes were kept aligned, but a 45° angle was placed in the vinyl tubing 4 mm distal to the renal arteries. Model C was designed to represent an ill-measured fenestrated graft and was straight, but the right renal hole was intentionally misplaced 5.6 mm ventral to the appropriate position, and the left renal hole was misplaced 5.6 mm cranial to the appropriate position. For each model, the fenestrated graft was deployed six times using 6F Ansel sheaths (Cook Medical) for alignment and six times using Mustang balloons (Boston Scientific, Marlborough, Mass) inflated to nominal pressure for alignment. A 7-mm balloon was used in the superior mesenteric artery hole and 6-mm balloons were used in the renal artery holes. Based on preliminary findings, all deployments were performed with upward traction placed on our deployment model during removal of the constraining wire. Percent area encroachment of graft material on target vessel ostium was calculated using image analysis software and compared with the Student *t*-test.

Results: In model A, average percentage of area encroachment when using sheaths for alignment was $6.4\% \pm 1.5\%$ compared with $5.8\% \pm 1.0\%$ for balloons ($P = .73$). In model B, average percentage area encroachment was $45.9\% \pm 7.8\%$ for sheaths compared with $20.6\% \pm 3.8\%$ for balloons ($P < .01$). The renal fenestration on the outer curve was responsible for the majority of the mal-alignment, with an average encroachment of 79% due to the fenestration opening distal to its intended site. In model C, average percentage area encroachment was $44.1\% \pm 3.4\%$ for sheaths compared with $13.3\% \pm 2.4\%$ for balloons ($P < .01$). For completeness, our preliminary findings using sheath alignment in model A with no upward traction during removal of the constraining wire resulted in an average percentage area encroachment of $25.3\% \pm 6.6\%$, leading us to alter our protocol to include upward traction during all deployments.

Conclusions: Our results provide some insight into the behavior of fenestrated grafts during the actual mechanism of deployment. Although sheaths appear adequate for alignment of fenestrations to target vessels in straightforward anatomy with precisely measured fenestrations and scallops, inflated balloons in our bench top model provide significant improvement in targeted vessel alignment in tortuous anatomy and in fenestrated grafts with inaccurately measured fenestrations and scallops. Because it is standard practice that balloons are inserted in the target vessels to aid tracking of the sheaths into the vessels, using these same balloons to improve alignment of the fenestrations would add little to the case. It should also be noted that adequate alignment using sheaths required upward pressure during removal of the constraining wire in our model. Although this finding may in part be due to the decreased axial support of the graft inherent in our deployment model, it also demonstrates the advantage of using the natural fulcrum of the femoral-based sheaths (or balloons) in the target vessels. Therefore, there is intuitive logic that this other simple maneuver can help to further improve alignment. Admittedly, while mal-alignment can be at least partially overcome using stents, it does require biomechanical forces to maintain proper alignment. This can lead to an acute or chronic stresses on the targeted vessel tangential to the fenestrated stent graft, which, in theory, may cause stent fracture or accelerated stent intimal hyperplasia that causes early or late stent occlusion. Certainly, there can be little disadvantage to improved initial alignment of the fenestrations and decreased chronic forces on the branch vessel stents. We believe that another very interesting finding of our study was that balloon alignment during deployment can also overcome intentional misplaced fenestrations. This is because there is excess material in the circumference of the graft compared with the smaller lumen of the aorta. By manipulating the excess material so that it is unevenly distributed

throughout its circumference, one can essentially move fenestration in multiple directions. The implications is that balloon alignment during deployment may extend the applicability of off-the-shelf designs to greater variations in anatomy. Finally, our results also suggest that renal fenestrations should likely be placed more proximal than expected during planning for vessels arising from the outer curve of angulated anatomy to compensate for the poor tilt that occurs because of the tortuosity.

Author Disclosures: N. T. Scherrer: Nothing to disclose; Z. J. Minion: Nothing to disclose; E. S. Xenos: Nothing to disclose; J. L. Bobadilla: Nothing to disclose; D. J. Minion: Nothing to disclose.

Flexible Robotics With Electromagnetic Tracking Improve Safety and Efficiency During In Vitro Endovascular Navigation



Adeline Schwein¹, Ben Kramer², Ponraj Chinna Durai³, Sean Walker⁴, Marcia O'Malley², Alan Lumsden¹, Jean Bismuth¹. ¹Houston Methodist Hospital, Houston, Tex; ²Rice University, Houston, Tex; ³Siemens Medical Solution USA, Inc, Hoffman Estates, Ill; ⁴Hansen Medical Inc, Mountain View, Calif

Background: One limitation of the remotely steerable robotic catheter (Magellan, Hansen Medical Inc, Mountain View, Calif) is the lack of real-time 3D localization: it is still being navigated based on 2D X-ray fluoroscopic projection images. Our goal was to evaluate if incorporating an electromagnetic (EM) sensor in the robotic catheter tip can overcome this limitation and potentially improve endovascular navigation.

Methods: Six users with varied experience in robotic endovascular procedures were tasked to navigate using the 9F robotic catheter, with EM sensors incorporated at the tip of leader, in a fluid-filled aortic aneurysm phantom. An EM field was generated by a device under the angiography table. All users cannulated two anatomical targets (left renal artery and a "gate" located towards the posterior aspect of the model) using 4 different visualization modes (Fig 1): (1) Standard fluoroscopy mode (control); (2) 2D biplane fluoroscopy mode showing real-time virtual catheter orientation from EM tracking; (3) 3D VRT model (AP view) of phantom and endoluminal view showing virtual catheter orientation from EM tracking; (4) 3D

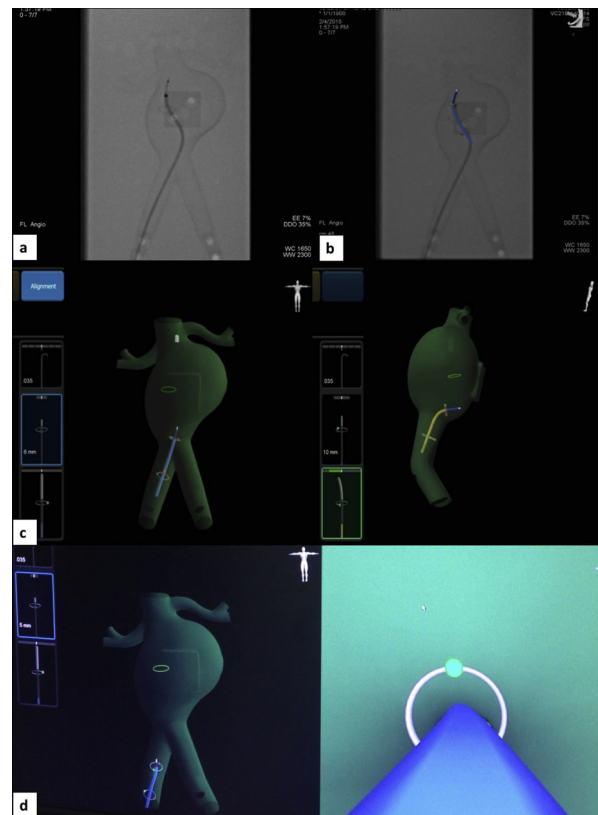


Fig.

Table. Average results for all performance parameters for both cannulation tasks and for each visualization mode. Comparison between mode 1 and the average of modes 2-3-4 was made for each parameter using a Student *t*-test

Variable	Mode 1	Mode 2	Mode 3	Mode 4	P
Fluoroscopy time, seconds	274	20	29	2	.001
Cannulation time (min:sec)	08:12	04:19	04:29	03:09	.013
3D pathway, mm	1043.4	445.8	441.0	417.2	.009
Spectral arc length	-13.8	-10.9	-9.5	-9.1	.017
Dimensionless jerk	612,924.0	315,650.2	219,863.1	217,938.8	.009
Number of submovements	37.2	19.7	19.5	15.5	.002

VRT model (AP and lateral view) showing virtual catheter orientation from EM tracking. Standard X-ray fluoroscopic imaging was always available. Cannulation and fluoroscopy times were noted for every mode. 3D positions of the tip sensor were recorded at 4 Hz to establish and measure catheter trajectories. Kinematic metrics, including number of submovements, spectral arc length, and dimensionless jerk, were calculated to assess the consistency of the catheter motion. A contrast *t*-test was used to compare standard fluoroscopy mode to the use of EM tracking.

Results: The EM sensor incorporated catheter navigated as expected according to all users. The success rate for cannulation was 100%. For the posterior gate target, mean cannulation times (minutes:seconds) were 8:12, 4:19, 4:29, and 3:09, respectively, for the modes 1, 2, 3, and 4 ($P = .013$). Mean fluoroscopy times were 274, 20, 29, and 2 seconds respectively ($P = .001$). Mean 3D path lengths were 1046, 446, 441, and 417 mm, respectively ($P = .009$). Spectral arc length, dimensionless jerk, and number of submovements were all significantly reduced when using EM tracking for the posterior gate cannulation ($P < .05$; Table), showing higher quality of movement.

Conclusions: The EM tracked Magellan robotic catheter allowed better real-time 3D orientation, facilitating navigation, with reduction in cannulation and fluoroscopy times and improvement in motion consistency. Although this is preliminary work, it has the potential to improve procedural safety and efficacy and to lead toward “fluoroscopy free” endovascular surgery.

Author Disclosures: A. Schwein: Nothing to disclose; B. Kramer: Nothing to disclose; P. Chinna Durai: Employee of Siemens Medical Solution USA Inc; S. Walker: Employee of Hansen Medical Inc; M. O'Malley: Nothing to disclose; A. Lumsden: Consultant for Hansen Medical Inc; J. Bismuth: Nothing to disclose.

AAA Repair in Octogenarians: Is it Worth the Risk?

Caitlin W. Hicks, Tammam Obeid, Isibor Arhuidese, Umair Qazi, Mahmoud B. Malas. Johns Hopkins Hospital, Baltimore, Md

Background: Age is a well-known independent risk factor for mortality after AAA repair. However, there is significant debate about the utility of AAA repair in older patients. We aimed to compare mortality outcomes after endovascular AAA repair (EVAR) and open AAA repair (OAR) in octogenarians (age ≥ 80 years) compared with younger patients (age < 80 years).

Methods: All patients recorded in the Vascular Quality Initiative database (2002-2012) who underwent infrarenal AAA repair were included. Univariable and multivariable statistics were used to compare perioperative (30-day) and 1-year mortality outcomes between octogenarians vs nonoctogenarians for both OAR and EVAR procedures.

Results: Overall, 21,874 patients underwent AAA repair during the study period (OAR, 5765; EVAR, 16,109), including 4839 octogenarians (OAR, 765; EVAR, 4074) and 17,035 nonoctogenarians (OAR, 5000; EVAR, 12,035). Octogenarians (mean age, 83.01 ± 0.09 years) were less frequently male (66% vs 75%) and had a higher prevalence of congestive heart disease (9.9% vs 7.1%), chronic renal insufficiency (12.2% vs 7.5%), and a history of prior aortic surgery (14.3% vs 7.7%) compared with nonoctogenarians ($P < .001$ for all). Intraoperative use of blood transfusions and vasopressors were more common in octogenarians for both OAR (blood: 3.3 ± 4.4 vs 1.8 ± 3.7 units; vasopressors: 45.2% vs 32.8%) and EVAR (blood: 0.43 ± 1.7 vs 0.31 ± 1.6 units; vasopressors: 7.6% vs 5.7%; $P < .001$ for all). Contrast volumes used during EVAR were similar between groups (108 ± 71 vs 107 ± 68 mL; $P = .18$). Perioperative mortality after OAR was 20.1% in the octogenarian group compared with 7.1% in nonoctogenarians ($P < .001$). Perioperative mortality after EVAR was 3.8% in the octogenarian group compared with 1.6% in nonoctogenarians ($P < .001$). One-year mortality among octogenarians vs nonoctogenarians was 24.8% vs 9.0% for OAR (Fig, A) and 11.6% vs 5.7% for EVAR (Fig, B), respectively (log-rank test $P < .001$ for both). Multivariable analysis controlling for

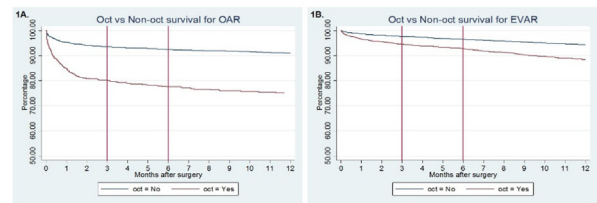


Fig.

baseline and intraoperative differences between groups demonstrated that age ≥ 80 years increased the risk of 30-day and 1-year mortality after AAA repair by 236% and 194%, respectively ($P < .001$ for both).

Conclusions: AAA repair should be approached with extreme caution in the octogenarian population. Perioperative and 1-year mortality rates after OAR are particularly high in this age group, suggesting that the risk associated with open surgery may outweigh the benefits in older patients.

Author Disclosures: C. W. Hicks: Nothing to disclose; T. Obeid: Nothing to disclose; I. Arhuidese: Nothing to disclose; U. Qazi: Nothing to disclose; M. B. Malas: Nothing to disclose.

Differential Hypertensive Protease Expression in the Thoracic Versus Abdominal Aorta

Jean Marie Ruddy, Adam W. Akerman, Denise Kimbrough, Elizabeth N. Nadeau, Stroud E. Robert, Rupak Mukherje, John S. Ikonomidis, Jeffrey A. Jones. Medical University of South Carolina, Charleston, SC

Background: Hypertension, which is a major risk factor for cardiovascular morbidity and mortality, can drive pathologic remodeling of the macro- and micro-circulation. Patterns of aortic pathology differ, however, suggesting regional heterogeneity of the pressure-sensitive protease systems triggering extracellular matrix remodeling in the thoracic aorta (TA) and abdominal aorta (AA). This study tested the hypothesis that the expression of two major protease systems (matrix metalloproteinases [MMPs], and cathepsins) in the TA and AA would be differentially affected with hypertension.

Methods: Normotensive (BPN/3) mice at age 14 to 16 weeks underwent implantation of osmotic infusion pumps for 28 day angiotensin II (BPN/3+AngII; $n = 3$) delivery (1.46 mg/kg/d) to induce hypertension. The TA and AA were harvested to determine levels of MMP-2, MMP-9, MT1-MMP, and cathepsins S, K, and L were evaluated in age-matched BPN/3 ($n = 8$), control, and BPH/2 spontaneously hypertensive mice (non-AngII pathway; $n = 4$). Blood pressure was monitored via CODA tail plethysmography. Quantitative RT-PCR and immunoblotting/zymography was used to measure MMP and cathepsin mRNA expression and protein abundance, respectively. All values in the hypertensive mice were compared using a one-sample *t*-test to control mice. In addition comparisons between the BPN/3+AngII and BPH/2 were made using a two-sample *t*-test.

Results: After 28 days of infusion, the BPN/3+AngII mice had a 17% increase in systolic blood pressure, matching that of the BPH/2 spontaneously hypertensive mice (both $P < .05$ vs control BPN/3). MMP-2 mRNA levels were elevated in TA and AA in BPH/2 as well as BPN/3+AngII mice but was further elevated in the TA of BPN/3+AngII mice, with a concordant increase in zymographic abundance ($P < .05$). MMP-9 mRNA was decreased in the TA of BPH/2 mice and in the AA of both experimental groups ($P < .05$ vs control). MT1-MMP mRNA trended up in the TA and down in the AA in both hypertensive models. Expression of cathepsins K and L was reduced in both aortic regions of BPH/2 mice ($P < .05$), with concordantly decreased protein abundance in the AA ($P < .05$). However, mRNA levels of cathepsins S, K, and L were increased in the TA of BPN/3+AngII mice compared with normotensive control mice ($P < .05$).

Conclusions: By using two different models of hypertension, this study has identified pressure-dependent as well as AngII-dependent regional alterations in aortic gene expression of MMPs and cathepsins that may lead to differential remodeling responses in each of the aortic regions. Further studies will delineate mechanisms and may provide targeted therapies to attenuate downstream aortic pathology based on demonstrated regional heterogeneity.

Author Disclosures: J. Ruddy: Honoraria, Medtronic Fellows Education; A. W. Akerman: Nothing to disclose; D. Kimbrough: Nothing to disclose; E. N. Nadeau: Nothing to disclose; S. E. Robert: Nothing to disclose; R. Mukherje: Nothing to disclose; J. S. Ikonomidis: Nothing to disclose; J. A. Jones: Nothing to disclose.